

## CFD Analysis on a Core Outlet Flow through the Fuel Alignment Plate of SMART

Y.I. Kim<sup>a\*</sup>, Y.M. Bae<sup>a</sup>, K.K. Kim<sup>a</sup>

<sup>a</sup>Korea Atomic Energy Research Institute, 1045 Daedeok Street, Yuseong-gu, Daejeon 3050353, Korea

\*Corresponding author: yikim3@kaeri.re.kr

### 1. Introduction

The flow distribution of an active core is one of the major concerns in a reactor design, as it is related to the fuel integrity in normal operation and accident condition. In an open core allowing a cross flow, the inlet flow condition mostly affects the overall flow distribution of the active core region. However, the outlet condition is not negligible as the condition also influences the flow uniformity near the outlet region of the active core. CFD (Computational Fluid Dynamics) simulations were performed to confirm the core flow distribution for SMART, which acquired standard design approval in 2012 [1~4]. In this paper, CFD simulation is also used to calculate the pressure distribution of a core outlet, a Fuel Alignment Plate (FAP), for SMART.

In SMART, the fluid discharged from the Steam Generator comes into a Flow Mixing Header Assembly (FMHA), and is rearranged and split into a very fine size. The FMHA is greatly important for enhancing the flow distribution of a downcomer during a normal operation, transient, and even accidents. Then, the fluid discharged from the FMHA flows into the core upstream through flow skirt holes. The Low Core Support Plate (LCSP) reallocates the flow introducing into the inlet core from the core upstream. The deviation of flow distribution becomes smaller or almost disappears by LCSP holes having relatively large loss coefficient compared to the downstream flow deviation. In an open core, the flow deviation at the core inlet region is diminished by cross flow as it goes upward. Near the core outlet, the flow distribution can be distorted by the influence of a Fuel Alignment Plate (FAP) installed above the fuels.

In this paper, the effect of the core outlet flow structure such as the FAP holes of SMART is investigated. Before the calculation, the influences of mesh size and turbulence models are inspected.

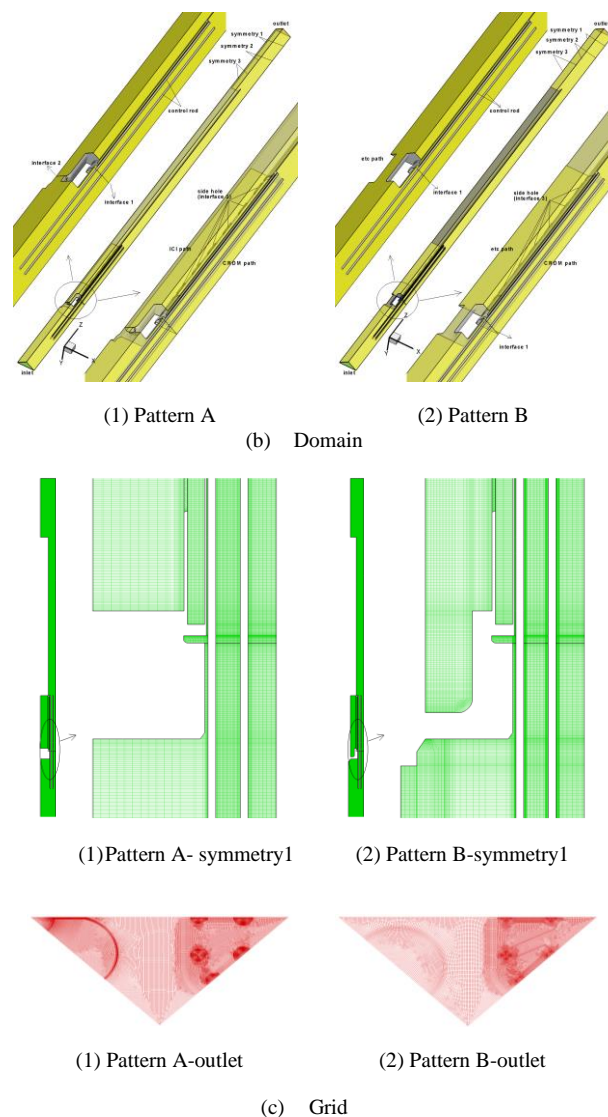
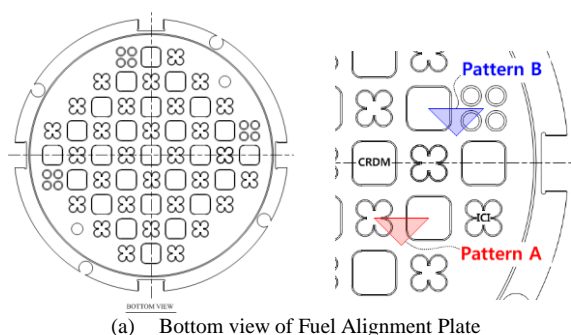


Fig. 1. Geometry, BC and grid of computational domain

### 2. Methods

#### 2.1 Model description

The steady, incompressible, and three-dimensional symmetric flow (Fig. 1) and constant properties are assumed in these CFD simulations using Fluent 12[5]. All simulations have been carried out with the 2<sup>nd</sup>-order upwind scheme for discretization, a single precision solver, the SIMPLE algorithm for pressure-velocity coupling, and the standard wall function for RKE



(a) Bottom view of Fuel Alignment Plate

(Realizable  $k-\varepsilon$ ) and RNG (Renormalization Group  $k-\varepsilon$ ) turbulence models. The low Reynolds correction option is not applied for SST (Shear Stress Transport  $k-\omega$ ).

The governing equations for the three dimensional incompressible steady and turbulent flow are as follows:

$$\frac{\partial \langle u_i \rangle}{\partial x_i} = 0 \quad (1)$$

$$\rho \frac{\partial \langle u_i \rangle \langle u_j \rangle}{\partial x_j} = -\frac{\partial \langle p \rangle}{\partial x_i} + \frac{\partial}{\partial x_j} \left[ \mu \left( \frac{\partial \langle u_i \rangle}{\partial x_j} + \frac{\partial \langle u_j \rangle}{\partial x_i} \right) - \rho \langle u_i u_j' \rangle \right] \quad (2)$$

Three kind of turbulence models, i.e., SST, RNG, and RKE, summarized in reference [5] are applied in this paper.

## 2.2 Code V&V

Before the main calculation for the core outlet flow, some validation calculations had been performed on a two dimensional axisymmetric flow through a chamfered orifice. Figure 2 shows the configuration, boundary conditions (BC), and grid. The domain has an inlet, an outlet and an axis.

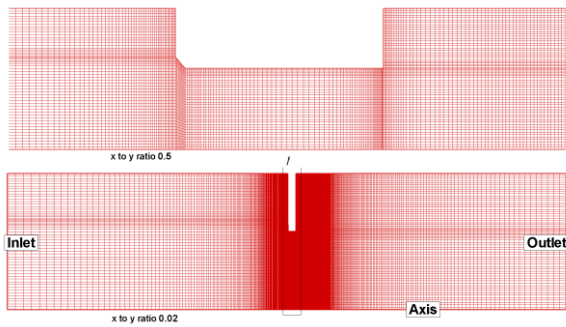


Fig. 2. Geometry, BC and grid for V & V

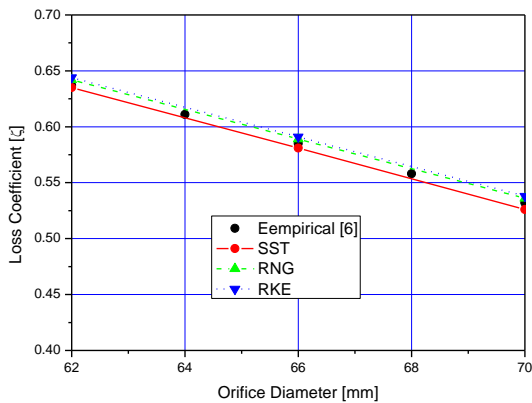


Fig. 3. Comparison an empirical correlation and the simulation result with turbulence models

To remove the effect of the inlet and outlet region, the length of the inlet and outlet regions is extended to approximately 50-times the outside diameter. The calculation results are displayed in Fig. 3. As shown in

this figure, the results of numerical simulations agree very well with an empirical correlation [6].

## 2.3 Configurations and Boundary Conditions

As shown in Fig. 1(a), the SMART core consists of 57 fuel assemblies each having  $17 \times 17$  fuel rods. The patterns of the FAP flow holes upon the fuel assemblies are approximately classified into two groups: “pattern A” including CRDM and ICI holes and “pattern B” including CRDM and ETC holes.

Many computational resources should be used to model the fuel assemblies. However, the discharging flow distribution from the assemblies has not much meaning to evaluate the FAP flow as it is finely separated among  $17 \times 17$  fuel rods and has almost a uniform distribution. To simplify the analyses and focus on the core outlet flow, the discharging condition from the fuel assemblies, inlet condition, is modeled using a uniform velocity in this study.

Figure 1(b) shows the computational configuration, boundary conditions, and Fig. 1(c) displays grids at the symmetry and outlet planes. The domain including the two  $1/8$  fuel assemblies of CRDM and ETC or ICI sides has an inlet and an outlet and three symmetries. The simulation cases for the pattern A (Case A1, A2) and pattern B (Case B1~B6) are summarized in Table I.

Table I: Simulation case summary

Case	Turb. model	Mesh (million)	Norm. P Loss(%)	Norm. flow rate		P Diff. with Case B3 (%)
				CRDM	ETC/ICI	
A1	RKE	27.6	12.58	1.015	0.985	-0.6
A2	RKE	27.6	14.71	0.932	1.068	16.2
B1	RKE	11.7	12.50	0.990	1.010	1.2
B2	RKE	21.2	12.57	0.993	1.007	0.7
B3	RKE	24.8	12.66	0.992	1.008	-
B4	SST	24.8	12.53	1.006	0.994	-1.0
B5	RNG	24.8	12.58	1.007	0.993	-0.6
B6	RKE	24.8	13.78	0.958	1.042	8.9

## 3. Results and Discussion

### 3.1 Grid dependency and turbulence models

The grid sensitivity and the difference between turbulence models are inspected for a FAP pattern B as a base work shown in detail in Reference [4]. The deviation between a coarsen grid Case B1 and a fine grid Case B3 is less than 1.5%, and the CFD results of RKE, RNG, and SST are within 1.0% deviation as shown in Table 1 [4]. Therefore, the effects of grids and turbulence models are negligible in this simulation. The velocity magnitude distribution contours at a symmetry plane are displayed in Fig. 4.

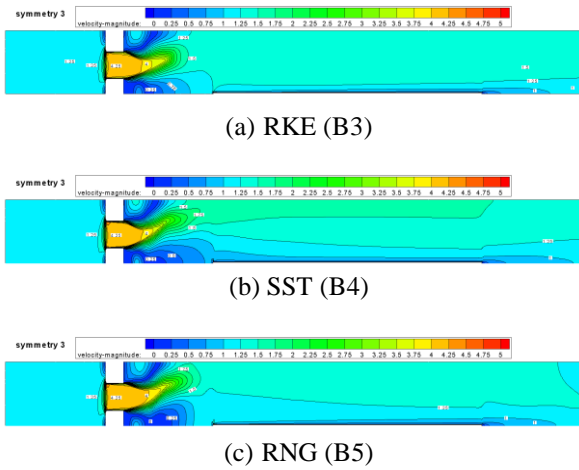


Fig. 4. Velocity magnitude contours of Case B3 to B5.

### 3.2 Effect of flow holes

Two FAP flow hole patterns having a similar flow resistance and even flow rate distribution to each flow path of CRDM and other side are simulated in Case B3 for pattern B and Case A1 for pattern A. Figure 5 shows the static pressure (1) and total pressure (2) variation along the centerline of individual paths. In this figure, the Z-axis end point means the FAP bottom of SMART. As shown in this figure, the pressure variation due to the FAP hole is negligible before the flow approaches very closely to the FAP. From this result, we can deduce that the FAP holes do not significantly affect the flow distribution near the outlet region of fuel assemblies.

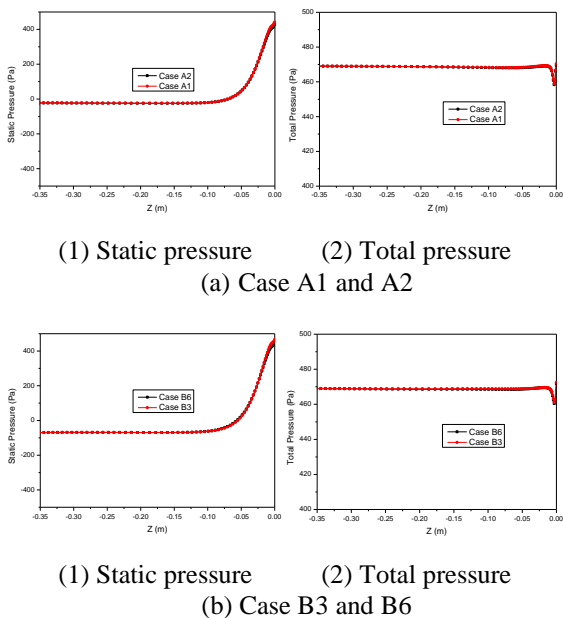


Fig. 5. Static and total pressure variation of Case A1, A2 and B3, B6.

### 3.3 Effect of uneven distribution of holes

To consider the effect of uneven distribution of mass flow rate between a CRDM side and other side holes,

Cases A2 and B6 showing different flow rates between two side holes are investigated. The static pressure (1) and total pressure (2) variations along the centerlines of the domains of Cases A1 & A2 and B3 & B6 are compared in Fig. 5. The shape difference between the cases with even and uneven flow distributions does not make any noticeable deviation for the axial pressure variation.

### 3.4 Effect of the distance to FAP

Figure 6 shows the pressure contours at some cross section in Cases A1 & A2 and B3 & B6. Figure 7 shows the static and total pressure distributions at a symmetric line of Fig. 6. The pressure distributions in Figs. 6 and 7 show almost the same distributions between two different cases respectively, and the distributions at approximately -5cm from the FAP bottom of Figs. 6 and 7 starts to change by the effect of the FAP.

From the investigation, we can deduce that a certain amount of pressure loss deviation between CRDM and other side does not produce any noticeable effect on the flow distribution near the outlet region of the fuel assemblies. However, we should not miss that this study is not for the global effect of all of FAP holes but for the local effect of a unit cell of FAP holes.

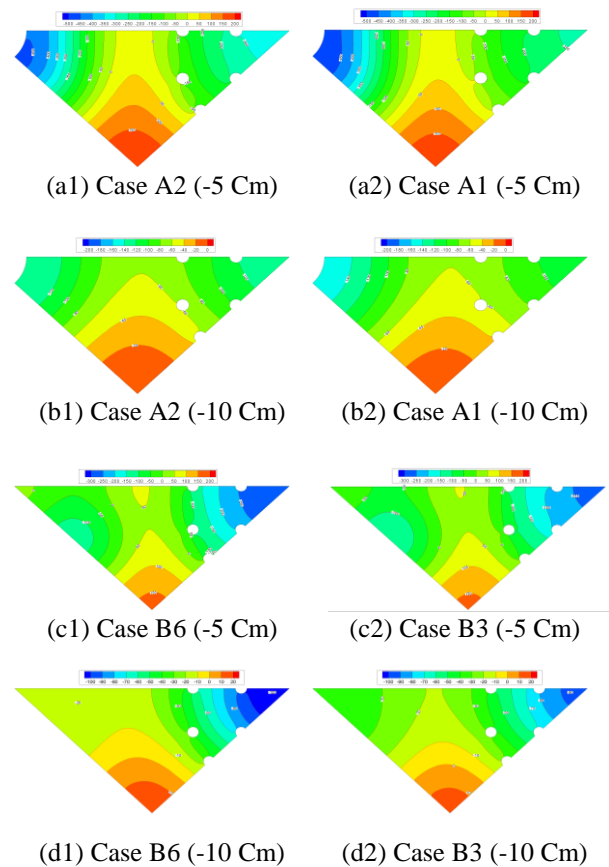


Fig. 6. Static pressure contours of Case A1, A2, B3 and B6.

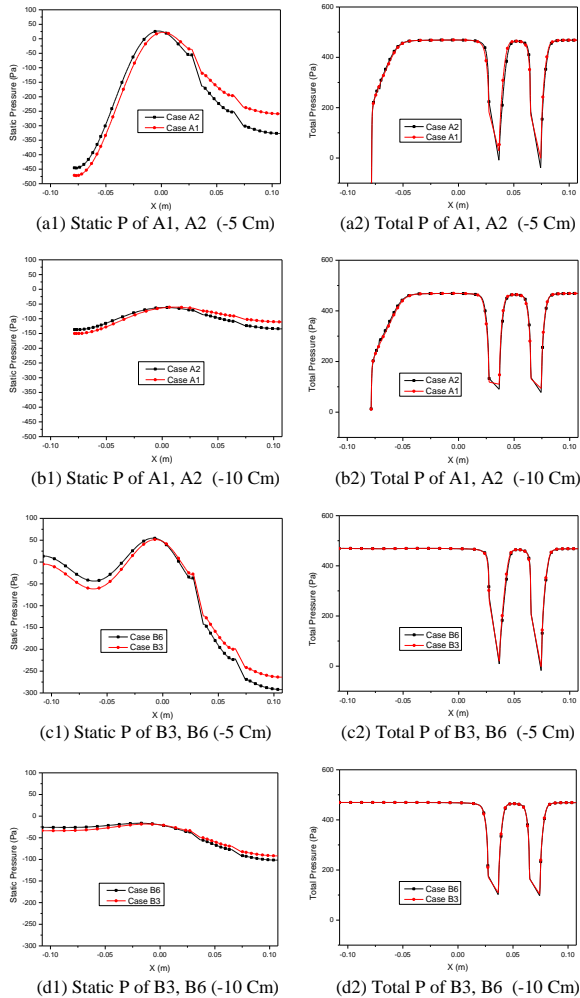


Fig. 7. Static pressure distribution at a symmetric line of Case A1, A2, B3 and B6.

#### 4. Conclusions

CFD simulations were performed to investigate the effect of FAP flow holes on the core outlet flow of SMART. As a preliminary study, the dependency of the mesh size and turbulence models was tested; a fine grid was applied, the effect of which is negligible, and the core outlet flow is not sensitive to the turbulence models.

In brief, the flow resistance of FAP is less than 15% of that of the fuel assemblies. The flow resistance deviation between two flow path patterns is less than 1% of that of active core. Even two flow path patterns located at the downstream location of the core outlet have a slightly different flow resistance, the deviation does not cause any significant variation of the core outlet flow near the fuel assemblies.

#### Acknowledgement

This work was supported by the National Research Foundation of Korea (NRF) funded by the Korea government (MSIP) (No. NRF-2012M2A8A4025974).

#### REFERENCES

- [1] Y.M. Bae, et.al., CFD Study on Flow Distribution at the Core Inlet Region of SMART, Trans. of KNS spring meeting, 2011.
- [2] Y.I. Kim, et.al., SMART Steam Generator Orifice Size Calculation, KAERI/100-NH301-003/2010, KAERI, 2010.
- [3] Y.I. Kim, Y.M. Jeon, Analysis on a Flow Resistance of Lower Core Support Plate in the SMART Reactor Flow Distribution Test, KAERI/100-TH301-016, KAERI, 2011.
- [4] Y.I. Kim, et.al., Flow Hole Size Calculation of Fuel Alignment Plate in SMART Reactor vessel, KAERI/100-NH301-018, KAERI, 2010.
- [5] Fluent 12.0 Manual, ANSYS Inc., 2009.
- [6] I.E. Idelchik, Handbook of Hydraulic Resistance, third edition, Begell house, 2000.